

Sunburst quantum Ising battery under periodic delta-kick charging

Ankita Mazumdar,^{1,2} Akash Mitra,^{1,2} and Shashi C. L. Srivastava^{1,2,*}

¹*Variable Energy Cyclotron Centre,
1/AF Bidhannagar, Kolkata 700064, India*

²*Homi Bhabha National Institute, Training School Complex,
Anushaktinagar, Mumbai - 400094, India*

Abstract

Most quantum batteries studied so far with notable exception of Sachdev-Ye-Kitaev (SYK) batteries are based on integrable models, where superlinear scaling of charging power—and hence a quantum advantage—can be achieved, but at the cost of unstable stored energy due to integrability. Here, by considering the sunburst quantum Ising battery driven by periodic delta-kicks, we show that in the quantum chaotic regime a quantum advantage is achieved for number of batteries $n_b \leq 4$, together with excellent stability of energy storage. In the integrable regime optimal energy storage and extraction are possible irrespective of the initial state of the charger. Finally, we show that the observed advantage does not originate from multipartite entanglement within the battery subsystem and is therefore classical in nature.

* Corresponding author : shashi@vecc.gov.in

I. INTRODUCTION

In recent times, there has been an upsurge of interest in the field of quantum thermodynamics, where fundamental thermodynamic principles such as energy transfer, storage, and work extraction processes are investigated at the quantum level [1–5]. The primary motivation has been to explore the role of quantum resources, such as coherence and entanglement, in enhancing the performance of different quantum thermodynamic devices, including quantum heat engines [6–11] and quantum batteries (QBs) [12–30]. Since the introduction of QBs by Alicki and Fannes [12], the possibility of realizing faster charging by utilizing the quantum entanglement has been investigated in details [13–15]. The global entangling operations, which enable the system to traverse a correlated shortcut in the associated Hilbert space causes the speed up in charging process [13, 14]. As a result, collective charging via global entangling unitary operations leads to a super-extensive scaling in charging power, known as the quantum advantage [31]. The first realization of quantum advantage in physically realizable models was shown in the Dicke QB [20], where the charging power per unit QB scales as \sqrt{N} , with N being the total number of QBs. The super-extensive scaling of charging power has also been observed in other models, including spin chain batteries [21–24, 32], central spin batteries [25–27] and Sachdev-Ye-Kitaev batteries [28, 29]. Recently, $\sqrt{N_c}$ quantum advantage in charging process with N_c number of chargers and single battery of the central spin QB has been experimentally verified in NMR systems [33].

Despite the presence of quantum advantage in the charging process, simultaneous optimization of extracted energy and charging power was not possible [20, 21, 34]. In the recently proposed sunburst quantum Ising battery [19], such simultaneous optimization became possible, together with the independence of both ergotropy—defined as the maximum amount of extracted energy via unitary operations—and charging power from the choice of the initial state. However, the charging power in this model was shown to scale only linearly with the number of batteries, indicating the absence of a quantum advantage. Although integrable models have been shown to provide quantum advantage in charging [27, 35, 36], they are unlikely to guarantee stability due to finite memory effects of the initial state, which induce rapid fluctuations in stored energy. It is also desirable for a QB not only to store the optimal amount of energy but also to allow complete extraction of the stored energy through unitary operations. In the case of a central spin QB, such optimization can be realized by

tuning the initial state of the charger, although this remains an experimentally challenging task [27].

The effect of periodically driven charging process of a QB, modelled by transverse Ising chain, with both transverse and longitudinal magnetic field, has been explored in Ref. [37]. Although global charging has been achieved in that setup, no quantum advantage in charging power was observed. The periodically driven charging protocol was further explored in Ref. [32], where it was shown that in the presence of both long-range interactions and a periodically driven charging, a superlinear scaling of charging power can be achieved in the long range XY model. There is a clear gap in current understanding of whether one can arrange optimal storage, quantum advantage, stability in the stored energy in a single model. Also, whether long range interactions are absolutely needed along with periodic driving to get the quantum advantage as has been the case in Ref. [32]? To address these, we investigate the sunburst quantum Ising battery [19] which involves only nearest neighbor interactions driven by periodic delta-kicks. We analyze the optimal energy storage and work extraction in this model of quantum battery numerically with some analytical results in limiting cases. We also demonstrate the stability of the energy storage and quantum advantage in the same model. Our results provide a unique situation where not only we achieve all the key markers of the quantum battery in the same model, we also demonstrate that quantum advantage can be arranged via periodic driving in short-range interacting models as well.

The paper is organized as follows. In Sec. II, we study the statistical properties of the model under periodic delta-kicks. In Sec. III, we study different limiting cases of the model where it is possible to realize optimal energy storage and work extraction. We show the stability of the energy storage and quantum advantage in periodic charging process in Sec. IV, and discuss the nature of advantage in Sec. V, while we present a conclusion in Sec. VI.

II. STATISTICAL PROPERTIES OF KICKED SUNBURST QUANTUM ISING MODEL

The sunburst quantum Ising model, which consists of a transverse field Ising chain symmetrically coupled to a few external isolated qubits, has been studied in the context of analyzing ground state properties [38] and entanglement dynamics under interaction quench

protocol [39]. Recently, this model has been explored as a quantum battery by considering the transverse Ising chain as a charger and external qubits as a quantum battery, known as the sunburst quantum Ising battery [19]. The Hamiltonian of this charger and battery is

$$H = H_c \otimes \mathbb{I}_b + \mathbb{I}_c \otimes H_b + \lambda(t)V_{cb}, \quad (1)$$

where H_c and H_b represent the Hamiltonian of the charger and battery, respectively. The interaction Hamiltonian is represented by V_{cb} , while \mathbb{I}_b (\mathbb{I}_c) represents the identity operator in the space of the battery (charger). Here, $\lambda(t)$ represents a time-dependent external control parameter, defining the charging protocol. The Hamiltonian for charger and the battery along with the interaction are expressed as

$$\begin{aligned} H_c &= - \sum_{i=1}^L (J\sigma_i^x \sigma_{i+1}^x + h\sigma_i^z) \\ H_b &= -\frac{\delta}{2} \sum_{i=1}^{n_b} \Sigma_i^z; \quad V_{cb} = -\kappa \sum_{i=1}^{n_b} \sigma_{1+(i-1)d}^x \Sigma_i^x, \end{aligned} \quad (2)$$

where L and n_b denote the number of Ising sites and external qubits, respectively. J is the strength of nearest neighbor interaction, which is assumed to be positive, i.e., $J > 0$ to ensure ferromagnetic interaction between the spins, and h is the transverse field strength. Furthermore, σ_i denotes the Pauli matrix on the i th Ising site, while Σ_i denotes the Pauli matrix corresponding to the i th battery. The energy gap between the two lowest eigenstates of the battery is represented as δ and κ represents the interaction strength between the battery and the charger. The distance between two consecutive qubits is denoted as d .

In this paper, we focus on the periodically driven charging protocol, specifically of the form

$$\lambda(t) = \sum_{n=-\infty}^{\infty} \delta\left(\frac{t}{\tau} - n\right), \quad (3)$$

where τ denotes the time period of charging Hamiltonian such that $\lambda(t + \tau) = \lambda(t)$. Such δ -kicked quench protocol can be realized with ultracold atoms exposed to a pulsed standing wave of near-resonant light [40]. It is worth noting that the above quench protocol differs from refs. [32, 37] where the periodic driving has a square wave form instead of a delta function impulse.

Given the periodic structure of the Hamiltonian in Eq. 1, i.e., $H(t + \tau) = H(t)$, the unitary operator U for one time-period describing the time evolution from just before to

just after the kick can be expressed in a factorized form as

$$U = e^{-iV_{cb}\tau} e^{-i(H_c \otimes \mathbb{I}_b + \mathbb{I}_c \otimes H_b)\tau} \quad (4)$$

$$= e^{-iV_{cb}\tau} [e^{-iH_c\tau} \otimes e^{-iH_b\tau}] \equiv U_{cb} (U_c \otimes U_b) , \quad (5)$$

where $U_c(U_b)$ governs the time evolution of charger (battery) alone in absence of the interaction while U_{cb} accounts for their instantaneous coupling via the interaction V_{cb} .

To understand the statistical properties of the quasi-energies ϕ_m and eigenvectors $|\psi_m\rangle$, defined by ,

$$U|\psi_m\rangle = e^{i\phi_m}|\psi_m\rangle. \quad (6)$$

of this Floquet system, we take resort to random matrix theory. The spacing distribution of consecutive energy levels is a widely used tool to distinguish integrable systems from classically chaotic ones. In chaotic systems, the level spacings typically follow the Wigner-Dyson distribution, whereas integrable systems exhibit a Poisson distribution [41–43]. The spacing between two consecutive unfolded quasi-energies is defined as

$$s_m = \frac{D}{2\pi} (\phi_{m+1} - \phi_m) , \quad (7)$$

where D the dimensionality of the Hilbert space [44]. The prefactor in the above equation ensures the unit mean spacing. If a system exhibits quantum chaos, both its eigenstates and eigenphases are expected to satisfy the predictions of random matrix theory (RMT). According to RMT, in the presence of time-reversal symmetry (Circular Orthogonal Ensemble), the nearest-neighbor level spacing distribution follows the Wigner-Dyson form:

$$P(s) = \frac{\pi}{2} s \exp\left(-\frac{\pi}{4} s^2\right). \quad (8)$$

The ratio of nearest neighbor spacing, \tilde{r}_n , another widely used quantity in RMT for its independence on unfolding scheme to study spectral fluctuation properties is defined as [45]

$$\tilde{r}_n = \frac{\min(s_n, s_{n-1})}{\max(s_n, s_{n-1})}. \quad (9)$$

The average value of the ratio of nearest neighbor spacing, $\langle \tilde{r} \rangle$, for the circular orthogonal ensemble takes the value $\langle \tilde{r} \rangle \approx 0.53$ while for integrable systems $\langle \tilde{r} \rangle \approx 0.38$ [46].

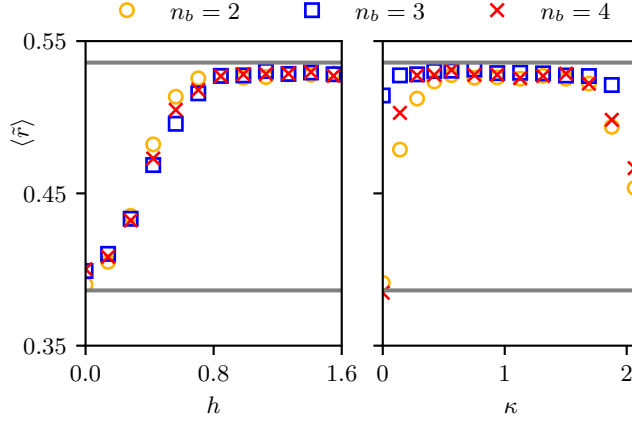


FIG. 1. (Left) The variation of $\langle \tilde{r} \rangle$ with h is plotted by keeping $J = \delta = \kappa = 1$ for three different number of batteries, $n_b = 2, 3, 4$. A clear transition from integrability for $h = 0$ to quantum chaotic nature for $h \approx 1$ is captured through average ratio of spacing. Two solid gray lines correspond to $\langle \tilde{r} \rangle \approx 0.386$ and $\langle \tilde{r} \rangle \approx 0.53$. (Right) Same is plotted with κ by keeping $J = \delta = h = 1$ for three different number of batteries, $n_b = 2, 3, 4$. The expected transition from integrability to chaos with increasing κ is clearly seen. The pronounced dip at $\kappa = 2$ is due to U_{cb} becoming a local operator (Eq. 10) which maps a direct product state to another direct product state.

Let's note that statistical features of a system are greatly affected by the presence of symmetries, and therefore, before comparing with RMT, one needs to either break all the discrete symmetries or compare the results for symmetry reduced operator. The translational symmetry and qubit exchange symmetry of the Floquet system are broken by randomizing the external magnetic field strength, h , and δ near the mean value. Since the Hamiltonian commutes with the parity operator, we restrict the unitary U to the even-parity sector. As we will see in the subsequent section, identifying the nature of the Hamiltonian H in Eq. 1—whether integrable or quantum chaotic—plays a pivotal role in understanding the performance of the QB and as the average values of ratio of spacings itself characterize the degree of chaos in the system satisfactorily, we plot $\langle \tilde{r}_n \rangle$ as a function of h and interaction strength κ in Fig. 1, by fixing (κ, δ) and $(h/J, \delta)$ respectively. In the limit $\kappa \rightarrow 0$, the system is in the integrable regime—this is expected since both subsystems, namely the transverse field Ising model and the external isolated qubits, are integrable. As previously reported in the case of the sunburst quantum Ising model with $\lambda(t) = 1$ [39], the total system approaches

the near integrable regime in the limit $h/J \ll 1$. However, with increasing κ and for $h/J \sim 1$, the system is in the quantum chaotic regime. Unlike the static case $\lambda(t) = 1$, under periodic delta-function impulses, the total system undergoes a rapid transition to the quantum chaotic regime even at relatively small interaction strengths, such as $\kappa \sim 0.2$. It is also worth noting that for $\kappa\tau = \pi/2$, $\langle \tilde{r} \rangle$ exhibits a sharp dip. This behavior can be understood from the structure of the unitary operator U_{cb} , which in this limit takes the form

$$U_{cb} = e^{i\frac{\pi}{2}(\sigma_{1+(i-1)d}^x \otimes \Sigma_i^x)} = i \prod_{i=1}^n \sigma_{1+(i-1)d}^x \otimes \Sigma_i^x. \quad (10)$$

It is evident from the above expression that U_{cb} simply flips all the Ising and qubit spins along the z direction. Any arbitrary state in the Hilbert space of the total system can be expressed as

$$|\Phi\rangle = \sum_{i=1}^{2^L} \sum_{j=1}^{2^{n_b}} \beta_{ij} |c_i\rangle \otimes |b_j\rangle, \quad (11)$$

where $|c_i\rangle, |b_j\rangle$ denote the i -th eigenstate of the transverse field Ising chain and the j -th eigenstate of external isolated qubits, respectively. It is easy to verify that if $|\Phi\rangle$ is an eigenstate of the unitary operator U in Eq. 4, then the coefficients β_{ij} must be identical for all j . This allows us to simplify the generic state $|\Phi\rangle$ to the form

$$|\Phi\rangle = \sum_{i=1}^{2^L} \beta_i |c_i\rangle \otimes \sum_{j=1}^{2^{n_b}} |b_j\rangle. \quad (12)$$

This shows that U_{cb} in eq. 10 acts as a local operator and fails to entangle the two subsystems. The above form of $|\Phi\rangle$ indicates that, for $\kappa\tau = \pi/2$, the eigenstates of U can be written as direct product states between the two individual subsystems. This, in turn, implies that for this specific value of κ , the total system effectively behaves as two decoupled non-interacting subsystems. Since both the individual subsystems are integrable, it is natural to expect that the total system exhibits integrable like behavior at $\kappa\tau = \pi/2$, which explains the observed dip in the average level spacing ratio $\langle \tilde{r} \rangle$ at $\kappa\tau = \pi/2$ as shown in Fig. 1.

III. OPTIMAL ENERGY STORAGE AND WORK EXTRACTION

Unlike most QB models that lie within the integrable regime, the sunburst quantum Ising battery subjected to periodic delta-kicks falls in the quantum chaotic regime (see Fig. [1]). This presents a significant challenge for obtaining an analytical insight about the

performance of this QB. However, as mentioned earlier, in the limit $h/J \ll 1$, the system makes a transition to the near integrable regime. This allows us to analytically evaluate various figures of merit related to the charging behavior of the QB and work extraction.

We consider the initial state of the total system as a direct product state between the individual ground states of the two subsystems. For $h = 0$, the ground state of the transverse field Ising model is the well-known “cat state” [47], also referred to as the Greenberger-Horne-Zeilinger state [48], given by $|\psi_G^I\rangle = \frac{1}{\sqrt{2}}[|++++\dots\rangle + |--\dots\rangle]$ with $\sigma_x |\pm\rangle = \pm |\pm\rangle$. We focus on the case of a single battery, so the initial state of the total system is $|\psi(0^-)\rangle = |\psi_G^I\rangle \otimes |0\rangle$, where $\Sigma_z |0\rangle = |0\rangle$. Acting with the interaction operator V_{cb} on $|\psi_G^I\rangle$ yields a new state $|\psi_N^I\rangle = \frac{1}{\sqrt{2}}[|++++\dots\rangle - |--\dots\rangle]$, which is orthogonal to $|\psi_G^I\rangle$. Applying V_{cb} once more on $|\psi_N^I\rangle$ returns the system to its original state $|\psi_G^I\rangle$. Both the states $|\psi_N^I\rangle$ and $|\psi_G^I\rangle$ are eigenstates of the Ising Hamiltonian H_c with same energy eigenvalue $-J$. As a result, $e^{-i(H_c \otimes \mathbb{I}_b)T}$ only produces a global phase factor and its effect can be ignored. This indicates that, in the limit $h \rightarrow 0$ and with only a single qubit, the dynamics produced by the unitary operator U becomes independent of the number of Ising sites. Therefore, we can perform our analytical calculation by considering the simplest situation where the number of Ising sites is only 2, i.e., $L = 2$. Moreover, the Hamiltonian commutes with the total parity operator, i.e., $[H, P] = 0$, where $P = \prod_{i=1}^L \sigma_i^z \otimes \prod_{j=1}^{n_b} \Sigma_j^z$. This allows us to restrict ourselves in either even sector ($P = +1$) or odd parity sector ($P = -1$). With these considerations, we choose the basis states as

$$\begin{cases} |\phi_0\rangle &= \frac{1}{\sqrt{2}}[|++\rangle + |--\rangle] \otimes |0\rangle \\ |\phi_1\rangle &= \frac{1}{\sqrt{2}}[|++\rangle - |--\rangle] \otimes |1\rangle \\ |\phi_2\rangle &= \frac{1}{\sqrt{2}}[|+-\rangle + |-+\rangle] \otimes |0\rangle \\ |\phi_3\rangle &= \frac{1}{\sqrt{2}}[|+-\rangle - |-+\rangle] \otimes |1\rangle \end{cases} \quad (13)$$

In this basis, the matrix corresponding to the unitary operator U becomes

$$U = \begin{bmatrix} \cos \kappa \tau e^{i\epsilon} & i \sin \kappa \tau e^{-i\epsilon} & 0 & 0 \\ i \sin \kappa \tau e^{i\epsilon} & \cos \kappa \tau e^{-i\epsilon} & 0 & 0 \\ 0 & 0 & \cos \kappa \tau e^{i\epsilon} & i \sin \kappa \tau e^{-i\epsilon} \\ 0 & 0 & i \sin \kappa \tau e^{i\epsilon} & \cos \kappa \tau e^{-i\epsilon} \end{bmatrix}, \quad (14)$$

where $\epsilon = \frac{\delta \tau}{2}$. The state $|\psi(n)\rangle$ after applying the n -th kick over the initial state $|\psi(0^-)\rangle$ can

be easily obtained as $|\psi(n)\rangle = F_n |\psi(0^-)\rangle$, where the matrix F_n is defined as $F_n = U^n$. Since the total system is always in a pure state, the density matrix of the full system becomes $\rho_{cb}^n = |\psi(n)\rangle\langle\psi(n)|$. By taking a partial trace over the charger degree of freedom, we obtain the reduced density matrix of the battery as

$$\rho_b^n = |(F_n)_{11}|^2 |0\rangle\langle 0| + |(F_n)_{21}|^2 |1\rangle\langle 1| \quad (15)$$

$$= (1 - |(F_n)_{21}|^2) |0\rangle\langle 0| + |(F_n)_{21}|^2 |1\rangle\langle 1|, \quad (16)$$

where $\sigma_z|1\rangle = -|1\rangle$ and

$$(F_n)_{21} = \frac{((e^{-i\epsilon}(a+b))^n - (e^{-i\epsilon}(a-b))^n)}{2^n b} i e^{2id} \sin \kappa\tau,$$

with, $a = 1 + e^{2i\epsilon} \cos \kappa\tau$, $b = \sqrt{a^2 - 4e^{2i\epsilon}}$

We now define a set of quantities that can be derived from the above expression of the reduced density matrix of the battery and will be necessary to analyze the performance of QB. The energy stored in the battery after applying n successive delta-kick is defined as

$$E(n) = \text{tr}(\rho_b^n H_b) - \text{tr}(\rho_b^0 H_b), \quad (17)$$

where ρ_b^0 is the density matrix of the battery corresponding to the initial state. Since we consider the initial state as the ground state of QB, we have $\text{tr}(\rho_b^0 H_B) = -\delta/2$. Thus, following Eq. 15 and Eq. 17, the expression for stored energy becomes

$$E(n) = \delta |(F_n)_{21}|^2. \quad (18)$$

Since $|(F_n)_{21}|_{\max}^2 = 1$, the maximum amount of energy that can be stored in the QB is δ , the energy gap between the ground state and excited state of the battery. This is referred to as the optimal energy storage. The another figure of merit of QB is the average charging power which quantifies the rate of charging in the QB and is defined at each stroboscopic time $t = n\tau$ as

$$P(n\tau) = E(n\tau)/n\tau. \quad (19)$$

The charging time is defined as the time when stored energy is maximized- if this happens after applying m successive kicks, then the charging time is simply $T = m\tau$. Under unitary cyclic transformation, not all the stored amount of energy can be extracted. The maximum

amount of useful energy that can be extracted from the state ρ_b^n via unitary transformation \tilde{U} is known as the ergotropy [49], and is defined as

$$\xi(\rho_b^n) = \text{tr}(\rho_b^n H_b) - \min_{\tilde{U}} \left\{ \text{tr} \left(\tilde{U} \rho_b^n \tilde{U}^\dagger H_b \right) \right\}, \quad (20)$$

where the minimization has to be performed over all the unitary transformations. It can be shown that the minimization is achieved when the state after the unitary transformation coincides with its passive counterpart [50], since any passive state $\tilde{\rho}_b^n$ satisfies the condition $\text{tr}(H_b \tilde{\rho}_b^n) \leq \text{tr}(H_b \tilde{U} \rho_b^n \tilde{U}^\dagger)$ for all unitaries \tilde{U} . As a result, no energy can be extracted from the passive state. The passive state $\tilde{\rho}_b^n$ must be diagonal in the eigenbasis of the Hamiltonian and its eigenvalues are the eigenvalues of ρ_b^n , but only in decreasing order. With these considerations, the ergotropy is expressed as

$$\xi(\rho_b^n) = \text{tr}(\rho_b^n H_b) - \text{tr}(\tilde{\rho}_b^n H_b). \quad (21)$$

It is easy to see that for a single battery unless the occupation probability corresponding to the ground state $|0\rangle$ does not exceed the occupation probability corresponding to the excited state $|1\rangle$, ergotropy is zero since the passive state counterpart of ρ_b^n coincides with the state ρ_b^n . The ergotropy is non-zero only when

$$|(F_n)_{11}|^2 < |(F_n)_{21}|^2 \implies |(F_n)_{21}|^2 > \frac{1}{2}, \quad (22)$$

or in other words population inversion occurs. If the above condition is satisfied, following Eq. 15, the expression of nonzero ergotropy is obtained as

$$\xi(\rho_b^n) = \delta \left(2|(F_n)_{21}|^2 - 1 \right). \quad (23)$$

Notice that optimal energy extraction—i.e., when the extracted energy equals the energy gap between the ground and the most excited state, $W(\rho_b^n) = \delta$ is possible only if $|F_{21}|^2 = 1$. This condition implies that the occupation probability of the excited state becomes unity, while that of the ground state vanishes. We further calculate the entanglement between the battery and charger to explore the effect of entanglement in extracting the amount of energy from the QB. Since the total system is always in a pure state, we use linear entropy to quantify the entanglement between battery and charger taken as two subsystems[19, 39]. The linear entropy of the QB is defined as

$$S_L(\rho_b^n) = 1 - \text{tr}(\rho_b^n)^2 = 2 \left(|(F_n)_{21}|^2 - |(F_n)_{21}|^4 \right) \quad (24)$$

As can be seen from Fig. 2, by tuning the parameters of the Hamiltonian in Eq. 1, under the periodic delta-kicks, it is possible to extract all possible energy that is stored in the battery, which is an important criterion for the best performance of the QB. For the special case where $\kappa\tau = \frac{\pi}{2}$, the reduced density matrix of the battery is simply $|0\rangle$ or $|1\rangle$ depending on the number of kicks being even or odd. Therefore, it is possible to realize optimal work extraction without producing any amount of entanglement between the battery and charger. However, this is a very special case where the coupled system behaves like two non-interacting subsystems. As it is shown in Fig. 2, it is also possible to simultaneously realize optimal energy storage and optimal work extraction from the QB for the other parameters as well when there is a finite amount of entanglement between the battery and charger. Specifically, in the limit $\kappa \gg \delta$, it is possible to realize both optimal energy storage and extraction. This is better than central spin model where optimal energy storage was realized only for a set of particular initial state of the charger [27]. In Fig. 2, by choosing the parameter $\kappa \gg \delta$, we numerically calculate the stored energy, ergotropy, and linear entropy and then compare the numerical values with the analytical expressions obtained in Eq. 18, Eq. 23 and Eq. 24, respectively. Interestingly, all the analytical expressions derived for $h = 0$ are in excellent agreement with the numerical values calculated for small yet finite $h(\sim 0.2)$. As can be seen from the figure, optimal energy can be stored and, at the same time, can be extracted without any waste of energy at regular intervals of time. At this point, the linear entropy between the battery and charger is minimized to a non-zero value. The optimal energy storage and work extraction are not confined to a single value of τ ; instead, they are realized over finite intervals of τ , specifically within the ranges $0.02 < \tau < 0.16$ and $0.18 < \tau < 0.35$ for fixed $\kappa = 6$. For the same choice of parameter regime, optimality in energy storage and extraction can be realized for a higher number of batteries too.

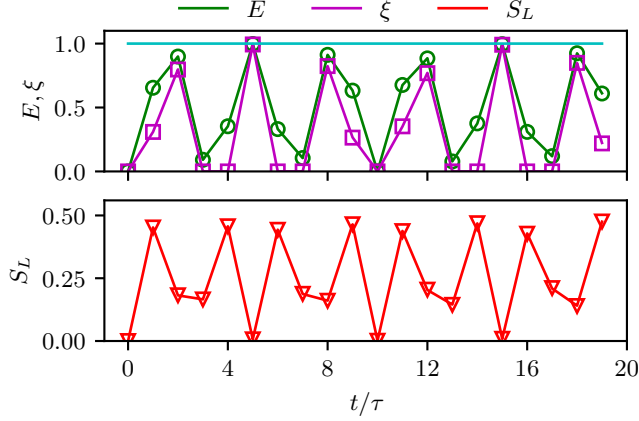


FIG. 2. The dynamics for E (green), ξ and S_L are plotted for the system size $L = 6$, $n_b = 1$ by keeping the parameters $J, \delta = 1$, $\kappa = 6$, $\tau = \pi/20$ and $h = 0.1$. The symbols stand for the numerical results and the solid lines are to show the analytical results derived in Eqs. 18, 23 and 24. The horizontal cyan line correspond to maximum possible stored energy, δ .

In this limiting case when $h/J \ll 1$, we do not find any quantum advantage since the maximum amount of entanglement between the battery and charger subsystems does not scale with the number of batteries, the maximum value is always $1/2$ irrespective of the number of batteries. As a result, the average charging power at the charging time scales only linearly with the number of batteries. Let us recall at this point that any superlinear scaling of average charging power with the number of QBs is dubbed as the quantum advantage [15]. Therefore, in this parameter regime, quantum advantage in the charging process can not be achieved. Furthermore, neither the energy storage nor ergotropy saturates around a fixed value; rather, they show an oscillating behavior. A good QB should provide optimal energy storage and extraction and, at the same time, should be able to provide stable energy storage without much fluctuation and produce a quantum advantage in the charging process. In the parameter regime $J \gg h$, the first criterion of producing a good QB is already achieved; however, the other two criteria are yet to be satisfied. In the next section, we investigate whether the remaining two criteria can be achieved in the sunburst quantum Ising battery under periodic delta-kicks by introducing a finite transverse field h , such that $J \sim h$.

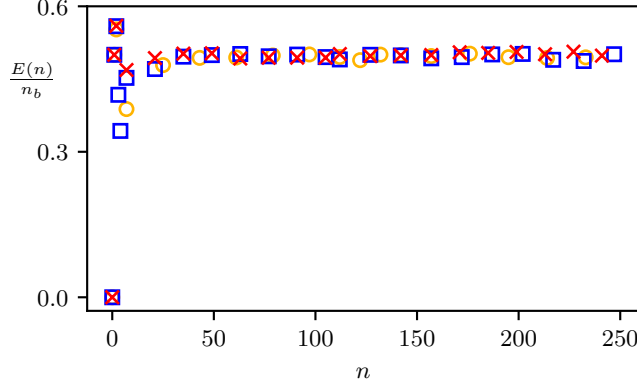


FIG. 3. The dynamics of $\frac{E(n)}{n_b}$ is shown for $n_b = 4$ (dark yellow), 5(blue) and 6(red). The total system sizes are chosen as $L + n_b = 13$ and the parameters are chosen as $J, h, \kappa, \delta = 1$ and $\tau = \pi/4$.

IV. STABLE ENERGY STORAGE AND QUANTUM ADVANTAGE

After achieving the near optimal energy storage and complete extraction of energy for work, we focus on stability of the energy storage[30, 51–53] as well as super-linear scaling of the average charging power, i.e, quantum advantage in this section. For other QB models, which mostly lie in the integrable regime, even though achieving super-linear scaling of charging power is possible, stable energy storage cannot be ensured [27, 35, 54]. As seen from the RMT studies of the sunburst quantum Ising battery under periodic delta-kicks, the model can be tuned from integrable to quantum chaotic regime. Therefore, we expect of achieving a stable energy storage from this battery by suitably choosing the parameters of the model to put it in chaotic regime. In the limit $J \simeq h$, we observe that the energy storage tends to saturate around a fixed value with negligible fluctuation (see Fig. 3). We use the standard deviation of time-series of $E(n)/n_b$ normalized by its mean value as the measure of temporal fluctuation of stored energy. The time-series starts from the charging time to $T = 250\tau$. For $n_b = 1$ to $n_b = 6$ with fixed $L + n_b = 13$, the values are found to be 0.07, 0.07, 0.05, 0.04, 0.03, and 0.03 respectively. Clearly, the energy storage becomes progressively more stable with increasing number of batteries. Even for a single battery, stability is very good.

Next we turn to study the possibility of obtaining quantum advantage in the charging process. For a classical battery, where no entanglement exists between the battery and charger, the stored energy scales linearly with the number of batteries, while the charging

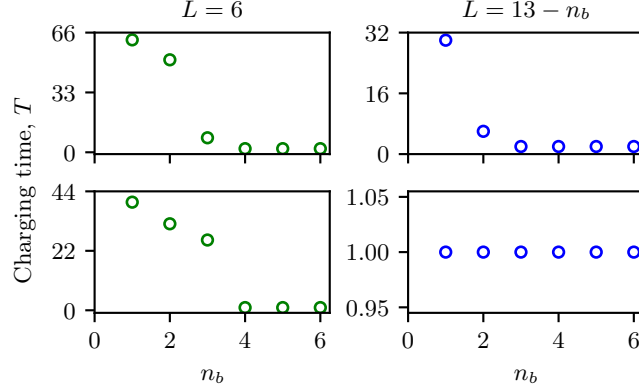


FIG. 4. The charging time is plotted against n_b in the left column for fixed charger length $L = 6$. The top-left curve corresponds to $\tau = \pi/4$ while the bottom-left correspond to $\tau = \pi/4 + 0.1$. The right column corresponds to scenario in which the total length of charger and battery is kept constant, 13 to be precise. Like in the left column case, top plot correspond to $\tau = \pi/4$ while bottom plot corresponds $\tau = \pi/4 + 0.1$. Other parameters are chosen as $J, h, \kappa, \delta = 1$.

time remains independent of it. Consequently, the charging power also scales linearly with the number of batteries. In the presence of finite entanglement between the battery and charger subsystems, the charging time can decrease with an increasing number of batteries. As the stored energy still scales linearly with the number of batteries, this reduction in charging time leads to a super-linear scaling of the average charging power. In Fig. 4, we plot the charging time as a function of the number of batteries. We observe that the charging power decreases as n_b increases from 1 to 4, and then saturates for $n_b > 4$, indicating the absence of quantum advantage beyond this point. However, for $n_b > 4$, the stored energy reaches its maximum immediately after two successive kicks. This implies that for larger n_b , the battery subsystem can reach the excited eigenstate more rapidly. We further ask whether, in the sunburst quantum Ising battery, maximum energy storage can be achieved immediately after the first kick, which would correspond to minimum charging time of the QB system. As shown in Fig. 4, this is indeed possible when the interval between successive kicks is chosen as $\tau \in [\pi/4 + 0.1, \pi/4 + 0.2]$. Moreover, for this choice of parameter, the quantum advantage for $n_b \leq 4$ remains intact.

V. NATURE OF ADVANTAGE

Having established the existence of quantum advantage in the previous section, we now investigate whether this advantage arises purely from the quantum correlations between the battery spins. In earlier literature on quantum batteries, the advantage has been classified into *genuine quantum advantage* and *classical advantage*, based on the source of the super-extensivity in the scaling of charging power with the number of batteries [15, 20, 27, 28, 35, 54–56]. If the super-extensivity arises due to the multipartite nature of the entanglement between the battery spins, the advantage is referred to as a genuine quantum advantage [28, 32, 54]. On the other hand, if it arises from the super-extensive scaling of the speed of evolution in energy eigenspace, the advantage is considered classical in nature. Based on the geometric framework, the average charging power $P(T)$ is bounded by [55],

$$P(T) \leq 2\sqrt{\langle \Delta H_b^2(t) \rangle_{t=T} \langle \Delta H^2(t) \rangle_{t=T}} \equiv P_{\text{bo}}(T), \quad (25)$$

where $\langle \Delta H_b^2(t) \rangle_{t=T}$ ($\langle \Delta H^2(t) \rangle_{t=T}$) denotes the time-average variance of the battery (total) Hamiltonian, evaluated at the charging time $T = m\tau$ and defined as

$$\langle \Delta H_b^2(t) \rangle_{t=T} = \frac{1}{T} \sum_{t=0}^{t=m\tau} \Delta H_b^2(t)|_{t=T}. \quad (26)$$

The time-average variance of the battery Hamiltonian can scale super-linearly with the number of batteries only in the presence of multipartite entanglement between the battery spins, whereas $\Delta H^2(t)$ determines the speed of evolution in energy eigenspace [55].

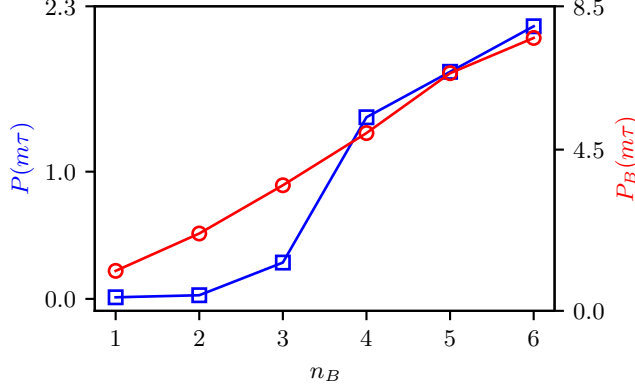


FIG. 5. Power from Eq: 19 (on the left y -axis) and the corresponding bound from Eq: 25 (on the right y -axis) have been plotted at the charging time ($m\tau$) with the n_b . A non-linear increase in power with increasing number of batteries is a clear signature of advantage over parallel classical charging scheme.

In Fig. 5, we show that the scaling of the charging power with the number of batteries does not follow the scaling of $P_{bo}(T)$. The charging power exhibits super-linear scaling with n_b for $n_b \leq 4$, whereas $P_{bo}(T)$ always scales linearly with n_b . This suggests that the bound in the average charging power derived in Eq. 25 is not tight enough to identify the origin of the super-linear scaling of the charging power [54]. Therefore, to determine whether the super-linear scaling of the charging power arises from quantum correlations—and thus a genuine quantum advantage—or from some other source which are not directly linked to the generation of multipartite entanglement between the battery spins (and hence a classical advantage), we calculate the quantum Fisher information, which quantifies the multipartite entanglement between the battery spins[27, 57–59].

We consider a generic mixed state of n_b qubits in its spectral decomposition

$$\rho = \sum_{i=1}^{2^{n_b}} \lambda_i |\lambda_i\rangle \langle \lambda_i|, \quad (27)$$

where $|\lambda_i\rangle$ are eigenvector of ρ with corresponding eigenvalue λ_i . For the state ρ , the quantum Fisher information is defined as [60–62]

$$F_Q[\rho, H] = 2 \sum_{i=1}^{2^{n_b}} \sum_{j=1}^{2^{n_b}} \frac{(\lambda_i - \lambda_j)^2}{(\lambda_i + \lambda_j)} \langle \lambda_i | \hat{S}^\alpha | \lambda_j \rangle \langle \lambda_j | \hat{S}^{\alpha'} | \lambda_i \rangle, \quad (28)$$

where $\hat{S}^\alpha = \frac{1}{2} \sigma^\alpha$ is the spin operator and $\alpha = \{x, y, z\}$. For the reduced time evolved state

of the battery, ρ_b^n , the multipartite entanglement between battery qubits is given by

$$F[\rho(t), \vec{n}, \vec{S}] \equiv \max_{|\vec{n}|=1} \vec{n}^T \Gamma \vec{n} \equiv \lambda_{\max}(\Gamma), \quad (29)$$

where \vec{n} is a unit vector on the Bloch sphere. The matrix Γ is introduced for maximization of $F[\rho(t), \vec{n}, \vec{S}]$ over measurement directions and its elements are defined as

$$\Gamma_{\alpha, \alpha'} = 2 \sum_{i,j} \frac{(\lambda_i - \lambda_j)^2}{(\lambda_i + \lambda_j)} \langle \lambda_i | \hat{S}^\alpha | \lambda_j \rangle \langle \lambda_j | \hat{S}^{\alpha'} | \lambda_i \rangle. \quad (30)$$

Here, $\lambda_{\max}(\Gamma)$ is the largest eigenvalue of Γ matrix. A multipartite entanglement witness is then obtained by the following condition:

$$\lambda_{\max}(\Gamma) > n_b. \quad (31)$$

n_b	$L = 6, \tau = \pi/4$	$L = 6, \tau = \pi/4 + 0.1$	$L = 13 - n_b, \tau = \pi/4$	$L = 13 - n_b, \tau = \pi/4 + 0.1$
2	0.287	0.047	0.219	0.191
3	0.205	0.082	0.187	0.410
4	1.395	0.278	0.262	1.202
5	0.664	2.942	1.220	0.587
6	2.260	4.655	1.099	1.531

TABLE I. Maximum eigenvalue $\lambda_{\max}(\Gamma)$ for various n_b , L , and τ values.

In Tab. I, we summarize the quantum Fisher information computed under two settings. First, we fix the number of Ising sites at $L = 6$ and vary the number of battery qubits $n_b = 2, \dots, 6$ for $\tau = \pi/4$ and $\tau = \pi/4 + 0.1$. Second, we fix the total system size $L + n_b = 13$ and again vary $n_b = 2, \dots, 6$ using the same two choices of τ . In every cases, we find that $\lambda_{\max}(\Gamma) < n_b$, indicating the absence of multipartite entanglement between the battery qubits. This allows us to conclude that, for the sunburst quantum Ising battery driven by periodic delta-kicks, the observed advantage in the charging process does not originate from multipartite entanglement and therefore does not constitute a genuine quantum advantage. Instead, the advantage is classical similar to what is observed in the central spin battery[27].

VI. CONCLUSION

In this paper, we have studied the performance of the sunburst quantum Ising battery under periodic delta-kicks. In the case of the interaction quench protocol, where the external

control parameter $\lambda(t)$ is a step function, the charging time does not depend on the number of batteries n_b . In contrast, under periodic delta-kicks the charging time decreases with increasing n_b for $n_b \leq 4$. This indicates a super-linear scaling of the charging power with n_b , thus signalling the presence of quantum advantage in the charging process. For $n_b > 4$, the stored energy reaches its maximum after the very first kick, implying near instantaneous charging in the presence of a large number of QBs. We further show that this quantum advantage does not originate from multipartite entanglement among the battery qubits and therefore is classical in nature. In contrast to commonly studied QB models that typically lie in the integrable regime, we show by analyzing the statistical properties within the framework of random matrix theory that the sunburst quantum Ising battery under periodic delta-kicks belongs to the quantum chaotic regime. Consequently, this battery can simultaneously provide stable energy storage along with quantum advantage. Although quantum advantage has been reported in many quantum batteries based on integrable models [21, 27, 54], these systems cannot naturally achieve stable energy storage due to integrability. Moreover, unlike the Sachdev–Ye–Kitaev battery [28, 30], the present model allows both quantum advantage and stable energy storage within the same parameter regime keeping only two body interaction. In the near-integrable regime, both optimal energy storage and energy extraction are possible irrespective of the charger’s initial state. This feature is absent in the central spin battery, where optimization can only be achieved for specific initial states of the charger [27]. In summary, the sunburst quantum Ising battery uniquely combines all three desired features of an efficient quantum battery—optimal energy storage and extraction, stable energy storage, and advantage in the charging process. To the best of our knowledge, these three features have not been found together in any other quantum battery model.

FUNDING

Open access funding provided by Department of Atomic Energy.

AUTHOR CONTRIBUTIONS

All authors contributed equally to the analysis, interpretation of the results and the preparation of the manuscript.

- ¹ Sai Vinjanampathy and Janet Anders. Quantum thermodynamics. *Contemporary Physics*, 57(4):545–579, July 2016. ISSN 1366-5812. doi:10.1080/00107514.2016.1201896. URL <http://dx.doi.org/10.1080/00107514.2016.1201896>.
- ² F. Binder, L.A. Correa, C. Gogolin, J. Anders, and G. Adesso. *Thermodynamics in the Quantum Regime: Fundamental Aspects and New Directions*. Fundamental Theories of Physics. Springer International Publishing, 2019. ISBN 9783319990460. URL <https://books.google.co.in/books?id=5uWPDwAAQBAJ>.
- ³ J. Gemmer, M. Michel, and G. Mahler. *Quantum Thermodynamics: Emergence of Thermodynamic Behavior Within Composite Quantum Systems*. Lecture Notes in Physics. Springer Berlin Heidelberg, 2009. ISBN 9783540705109. URL <https://books.google.co.in/books?id=Ua5tCQAAQBAJ>.
- ⁴ John Goold, Marcus Huber, Arnau Riera, Lidia del Rio, and Paul Skrzypczyk. The role of quantum information in thermodynamics—a topical review. *Journal of Physics A: Mathematical and Theoretical*, 49(14):143001, feb 2016. doi:10.1088/1751-8113/49/14/143001. URL <https://dx.doi.org/10.1088/1751-8113/49/14/143001>.
- ⁵ Manabendra Nath Bera, Arnau Riera, Maciej Lewenstein, Zahra Baghali Khanian, and Andreas Winter. Thermodynamics as a Consequence of Information Conservation. *Quantum*, 3:121, February 2019. ISSN 2521-327X. doi:10.22331/q-2019-02-14-121. URL <https://doi.org/10.22331/q-2019-02-14-121>.
- ⁶ Ronnie Kosloff and Amikam Levy. Quantum heat engines and refrigerators: Continuous devices. *Annual Review of Physical Chemistry*, 65(Volume 65, 2014):365–393, 2014. ISSN 1545-1593. doi:https://doi.org/10.1146/annurev-physchem-040513-103724. URL <https://www.annualreviews.org/content/journals/10.1146/annurev-physchem-040513-103724>.
- ⁷ Marlan O. Scully, M. Suhail Zubairy, Girish S. Agarwal, and Herbert Walther. Extracting work from a single heat bath via vanishing quantum coherence. *Science*, 299(5608):862–

- 864, 2003. doi:10.1126/science.1078955. URL <https://www.science.org/doi/abs/10.1126/science.1078955>.
- ⁸ Ting Zhang, Wei-Tao Liu, Ping-Xing Chen, and Cheng-Zu Li. Four-level entangled quantum heat engines. *Phys. Rev. A*, 75:062102, Jun 2007. doi:10.1103/PhysRevA.75.062102. URL <https://link.aps.org/doi/10.1103/PhysRevA.75.062102>.
 - ⁹ Hao Wang, Sanqiu Liu, and Jizhou He. Thermal entanglement in two-atom cavity qed and the entangled quantum otto engine. *Phys. Rev. E*, 79:041113, Apr 2009. doi:10.1103/PhysRevE.79.041113. URL <https://link.aps.org/doi/10.1103/PhysRevE.79.041113>.
 - ¹⁰ Kenza Hammam, Yassine Hassouni, Rosario Fazio, and Gonzalo Manzano. Optimizing autonomous thermal machines powered by energetic coherence. *New Journal of Physics*, 23(4):043024, apr 2021. doi:10.1088/1367-2630/abeb47. URL <https://dx.doi.org/10.1088/1367-2630/abeb47>.
 - ¹¹ Nathan M. Myers, Obinna Abah, and Sebastian Deffner. Quantum thermodynamic devices: From theoretical proposals to experimental reality. *AVS Quantum Science*, 4(2):027101, 04 2022. ISSN 2639-0213. doi:10.1116/5.0083192. URL <https://doi.org/10.1116/5.0083192>.
 - ¹² Robert Alicki and Mark Fannes. Entanglement boost for extractable work from ensembles of quantum batteries. *Phys. Rev. E*, 87:042123, Apr 2013. doi:10.1103/PhysRevE.87.042123. URL <https://link.aps.org/doi/10.1103/PhysRevE.87.042123>.
 - ¹³ Karen V. Hovhannisyanyan, Martí Perarnau-Llobet, Marcus Huber, and Antonio Acín. Entanglement generation is not necessary for optimal work extraction. *Phys. Rev. Lett.*, 111:240401, Dec 2013. doi:10.1103/PhysRevLett.111.240401. URL <https://link.aps.org/doi/10.1103/PhysRevLett.111.240401>.
 - ¹⁴ Felix C Binder, Sai Vinjanampathy, Kavan Modi, and John Goold. Quantacell: powerful charging of quantum batteries. *New Journal of Physics*, 17(7):075015, jul 2015. doi:10.1088/1367-2630/17/7/075015. URL <https://dx.doi.org/10.1088/1367-2630/17/7/075015>.
 - ¹⁵ Francesco Campaioli, Felix A Pollock, Felix C Binder, Lucas Céleri, John Goold, Sai Vinjanampathy, and Kavan Modi. Enhancing the charging power of quantum batteries. *Physical Review Letters*, 118(15), April 2017. ISSN 0031-9007. doi:10.1103/PhysRevLett.118.150601.
 - ¹⁶ Gian Marcello Andolina, Maximilian Keck, Andrea Mari, Michele Campisi, Vittorio Giovannetti, and Marco Polini. Extractable work, the role of correlations, and asymp-

- otic freedom in quantum batteries. *Phys. Rev. Lett.*, 122:047702, Feb 2019. doi: 10.1103/PhysRevLett.122.047702. URL <https://link.aps.org/doi/10.1103/PhysRevLett.122.047702>.
- ¹⁷ Gian Marcello Andolina, Maximilian Keck, Andrea Mari, Vittorio Giovannetti, and Marco Polini. Quantum versus classical many-body batteries. *Phys. Rev. B*, 99:205437, May 2019. doi:10.1103/PhysRevB.99.205437. URL <https://link.aps.org/doi/10.1103/PhysRevB.99.205437>.
 - ¹⁸ Hai-Long Shi, Shu Ding, Qing-Kun Wan, Xiao-Hui Wang, and Wen-Li Yang. Entanglement, coherence, and extractable work in quantum batteries. *Phys. Rev. Lett.*, 129:130602, Sep 2022. doi: 10.1103/PhysRevLett.129.130602. URL <https://link.aps.org/doi/10.1103/PhysRevLett.129.130602>.
 - ¹⁹ Akash Mitra and Shashi C. L. Srivastava. Sunburst quantum ising battery. *Phys. Rev. A*, 110: 012227, Jul 2024. doi:10.1103/PhysRevA.110.012227. URL <https://link.aps.org/doi/10.1103/PhysRevA.110.012227>.
 - ²⁰ Dario Ferraro, Michele Campisi, Gian Marcello Andolina, Vittorio Pellegrini, and Marco Polini. High-power collective charging of a solid-state quantum battery. *Phys. Rev. Lett.*, 120:117702, Mar 2018. doi:10.1103/PhysRevLett.120.117702. URL <https://link.aps.org/doi/10.1103/PhysRevLett.120.117702>.
 - ²¹ Thao P. Le, Jesper Levinsen, Kavan Modi, Meera M. Parish, and Felix A. Pollock. Spin-chain model of a many-body quantum battery. *Phys. Rev. A*, 97:022106, Feb 2018. doi:10.1103/PhysRevA.97.022106. URL <https://link.aps.org/doi/10.1103/PhysRevA.97.022106>.
 - ²² Fu-Quan Dou, Hang Zhou, and Jian-An Sun. Cavity heisenberg-spin-chain quantum battery. *Phys. Rev. A*, 106:032212, Sep 2022. doi:10.1103/PhysRevA.106.032212. URL <https://link.aps.org/doi/10.1103/PhysRevA.106.032212>.
 - ²³ Srijon Ghosh, Titas Chanda, and Aditi Sen(De). Enhancement in the performance of a quantum battery by ordered and disordered interactions. *Phys. Rev. A*, 101:032115, Mar 2020. doi: 10.1103/PhysRevA.101.032115. URL <https://link.aps.org/doi/10.1103/PhysRevA.101.032115>.
 - ²⁴ Srijon Ghosh, Titas Chanda, Shiladitya Mal, and Aditi Sen(De). Fast charging of a quantum battery assisted by noise. *Phys. Rev. A*, 104:032207, Sep 2021. doi:10.1103/PhysRevA.104.032207.

- URL <https://link.aps.org/doi/10.1103/PhysRevA.104.032207>.
- ²⁵ Li Peng, Wen-Bin He, Stefano Chesi, Hai-Qing Lin, and Xi-Wen Guan. Lower and upper bounds of quantum battery power in multiple central spin systems. *Phys. Rev. A*, 103:052220, May 2021. doi:10.1103/PhysRevA.103.052220. URL <https://link.aps.org/doi/10.1103/PhysRevA.103.052220>.
 - ²⁶ Jia-Xuan Liu, Hai-Long Shi, Yun-Hao Shi, Xiao-Hui Wang, and Wen-Li Yang. Entanglement and work extraction in the central-spin quantum battery. *Phys. Rev. B*, 104:245418, Dec 2021. doi:10.1103/PhysRevB.104.245418. URL <https://link.aps.org/doi/10.1103/PhysRevB.104.245418>.
 - ²⁷ Hui-Yu Yang, Kun Zhang, Xiao-Hui Wang, and Hai-Long Shi. Optimal energy storage and collective charging speedup in the central-spin quantum battery. *Phys. Rev. B*, 111:085410, Feb 2025. doi:10.1103/PhysRevB.111.085410. URL <https://link.aps.org/doi/10.1103/PhysRevB.111.085410>.
 - ²⁸ Davide Rossini, Gian Marcello Andolina, Dario Rosa, Matteo Carrega, and Marco Polini. Quantum advantage in the charging process of sachdev-ye-kitaev batteries. *Phys. Rev. Lett.*, 125:236402, Dec 2020. doi:10.1103/PhysRevLett.125.236402. URL <https://link.aps.org/doi/10.1103/PhysRevLett.125.236402>.
 - ²⁹ Gianluca Francica. Quantum advantage in batteries for sachdev-ye-kitaev interactions. *Phys. Rev. A*, 110:062209, Dec 2024. doi:10.1103/PhysRevA.110.062209. URL <https://link.aps.org/doi/10.1103/PhysRevA.110.062209>.
 - ³⁰ Dario Rosa, Davide Rossini, Gian Marcello Andolina, Marco Polini, and Matteo Carrega. Ultra-stable charging of fast-scrambling syk quantum batteries. *Journal of High Energy Physics*, 2020 (11), November 2020. ISSN 1029-8479. doi:10.1007/jhep11(2020)067. URL [http://dx.doi.org/10.1007/JHEP11\(2020\)067](http://dx.doi.org/10.1007/JHEP11(2020)067).
 - ³¹ Francesco Campaioli, Stefano Gherardini, James Q. Quach, Marco Polini, and Gian Marcello Andolina. Colloquium: Quantum batteries. *Rev. Mod. Phys.*, 96:031001, Jul 2024. doi:10.1103/RevModPhys.96.031001. URL <https://link.aps.org/doi/10.1103/RevModPhys.96.031001>.
 - ³² Stavva Puri, Tanoy Kanti Konar, Leela Ganesh Chandra Lakkaraju, and Aditi Sen De. Floquet driven long-range interactions induce super-extensive scaling in quantum battery, 2024. URL <https://arxiv.org/abs/2412.00921>.

- ³³ Jitendra Joshi and T. S. Mahesh. Experimental investigation of a quantum battery using star-topology nmr spin systems. *Phys. Rev. A*, 106:042601, Oct 2022. doi: 10.1103/PhysRevA.106.042601. URL <https://link.aps.org/doi/10.1103/PhysRevA.106.042601>.
- ³⁴ Gian Marcello Andolina, Donato Farina, Andrea Mari, Vittorio Pellegrini, Vittorio Giovannetti, and Marco Polini. Charger-mediated energy transfer in exactly solvable models for quantum batteries. *Phys. Rev. B*, 98:205423, Nov 2018. doi:10.1103/PhysRevB.98.205423. URL <https://link.aps.org/doi/10.1103/PhysRevB.98.205423>.
- ³⁵ Riccardo Grazi, Fabio Cavaliere, Maura Sassetti, Dario Ferraro, and Niccolò Traverso Ziani. Charging free fermion quantum batteries. *Chaos, Solitons & Fractals*, 196:116383, July 2025. ISSN 0960-0779. doi:10.1016/j.chaos.2025.116383. URL <http://dx.doi.org/10.1016/j.chaos.2025.116383>.
- ³⁶ Thao P. Le, Jesper Levinsen, Kavan Modi, Meera M. Parish, and Felix A. Pollock. Spin-chain model of a many-body quantum battery. *Phys. Rev. A*, 97:022106, Feb 2018. doi:10.1103/PhysRevA.97.022106. URL <https://link.aps.org/doi/10.1103/PhysRevA.97.022106>.
- ³⁷ Saikat Mondal and Sourav Bhattacharjee. Periodically driven many-body quantum battery. *Phys. Rev. E*, 105:044125, Apr 2022. doi:10.1103/PhysRevE.105.044125. URL <https://link.aps.org/doi/10.1103/PhysRevE.105.044125>.
- ³⁸ Alessio Franchi, Davide Rossini, and Ettore Vicari. Quantum many-body spin rings coupled to ancillary spins: The sunburst quantum ising model. *Phys. Rev. E*, 105:054111, May 2022. doi: 10.1103/PhysRevE.105.054111. URL <https://link.aps.org/doi/10.1103/PhysRevE.105.054111>.
- ³⁹ Akash Mitra and Shashi C. L. Srivastava. Sunburst quantum ising model under interaction quench: Entanglement and role of initial state coherence. *Phys. Rev. E*, 108:054114, Nov 2023. doi:10.1103/PhysRevE.108.054114. URL <https://link.aps.org/doi/10.1103/PhysRevE.108.054114>.
- ⁴⁰ F. L. Moore, J. C. Robinson, C. F. Bharucha, Bala Sundaram, and M. G. Raizen. Atom optics realization of the quantum δ -kicked rotor. *Phys. Rev. Lett.*, 75:4598–4601, Dec 1995. doi:10.1103/PhysRevLett.75.4598. URL <https://link.aps.org/doi/10.1103/PhysRevLett.75.4598>.

- ⁴¹ O. Bohigas, M. J. Giannoni, and C. Schmit. Characterization of chaotic quantum spectra and universality of level fluctuation laws. *Phys. Rev. Lett.*, 52:1–4, Jan 1984. doi:10.1103/PhysRevLett.52.1. URL <https://link.aps.org/doi/10.1103/PhysRevLett.52.1>.
- ⁴² Fritz Haake. *Quantum Signatures of Chaos*, pages 583–595. Springer US, Boston, MA, 1991. ISBN 978-1-4899-3698-1. doi:10.1007/978-1-4899-3698-1_38. URL https://doi.org/10.1007/978-1-4899-3698-1_38.
- ⁴³ Michael Victor Berry and M. Tabor. Level clustering in the regular spectrum. *Proceedings of the Royal Society of London. A. Mathematical and Physical Sciences*, 356(1686):375–394, 1977. doi:10.1098/rspa.1977.0140. URL <https://royalsocietypublishing.org/doi/abs/10.1098/rspa.1977.0140>.
- ⁴⁴ Tabea Herrmann, Maximilian F. I. Kieler, and Arnd Bäcker. Characterizing quantum chaoticity of kicked spin chains. *Phys. Rev. E*, 108:044213, Oct 2023. doi:10.1103/PhysRevE.108.044213. URL <https://link.aps.org/doi/10.1103/PhysRevE.108.044213>.
- ⁴⁵ Vadim Oganessian and David A. Huse. Localization of interacting fermions at high temperature. *Phys. Rev. B*, 75:155111, Apr 2007. doi:10.1103/PhysRevB.75.155111. URL <https://link.aps.org/doi/10.1103/PhysRevB.75.155111>.
- ⁴⁶ Y. Y. Atas, E. Bogomolny, O. Giraud, and G. Roux. Distribution of the ratio of consecutive level spacings in random matrix ensembles. *Phys. Rev. Lett.*, 110:084101, Feb 2013. doi:10.1103/PhysRevLett.110.084101. URL <https://link.aps.org/doi/10.1103/PhysRevLett.110.084101>.
- ⁴⁷ E. Schrödinger. Die gegenwärtige situation in der quantenmechanik. *Naturwissenschaften*, 23(49):823–828, Dec 1935. ISSN 1432-1904. doi:10.1007/BF01491914. URL <https://doi.org/10.1007/BF01491914>.
- ⁴⁸ Daniel M. Greenberger, Michael A. Horne, and Anton Zeilinger. Going beyond bell’s theorem, 2007.
- ⁴⁹ A. E. Allahverdyan, R. Balian, and Th. M. Nieuwenhuizen. Maximal work extraction from finite quantum systems. *Europhysics Letters*, 67(4):565, aug 2004. doi:10.1209/epl/i2004-10101-2. URL <https://dx.doi.org/10.1209/epl/i2004-10101-2>.
- ⁵⁰ Wiesław Pusz and Stanislaw Woronowicz. Passive states and kms states for general quantum systems. *Communications in Mathematical Physics*, 58:273–290, 10 1978. doi:10.1007/BF01614224.

- ⁵¹ Alan C. Santos, Barış Çakmak, Steve Campbell, and Nikolaj T. Zinner. Stable adiabatic quantum batteries. *Phys. Rev. E*, 100:032107, Sep 2019. doi:10.1103/PhysRevE.100.032107. URL <https://link.aps.org/doi/10.1103/PhysRevE.100.032107>.
- ⁵² Stefano Gherardini, Francesco Campaioli, Filippo Caruso, and Felix C. Binder. Stabilizing open quantum batteries by sequential measurements. *Phys. Rev. Res.*, 2:013095, Jan 2020. doi:10.1103/PhysRevResearch.2.013095. URL <https://link.aps.org/doi/10.1103/PhysRevResearch.2.013095>.
- ⁵³ Y. Yao and X. Q. Shao. Stable charging of a rydberg quantum battery in an open system. *Phys. Rev. E*, 104:044116, Oct 2021. doi:10.1103/PhysRevE.104.044116. URL <https://link.aps.org/doi/10.1103/PhysRevE.104.044116>.
- ⁵⁴ Gian Marcello Andolina, Vittoria Stanzione, Vittorio Giovannetti, and Marco Polini. Genuine quantum advantage in anharmonic bosonic quantum batteries. *Phys. Rev. Lett.*, 134:240403, Jun 2025. doi:10.1103/kzvn-dj7v. URL <https://link.aps.org/doi/10.1103/kzvn-dj7v>.
- ⁵⁵ Sergi Julià-Farré, Tymoteusz Salamon, Arnau Riera, Manabendra N. Bera, and Maciej Lewenstein. Bounds on the capacity and power of quantum batteries. *Phys. Rev. Res.*, 2:023113, May 2020. doi:10.1103/PhysRevResearch.2.023113. URL <https://link.aps.org/doi/10.1103/PhysRevResearch.2.023113>.
- ⁵⁶ Lei Gao, Chen Cheng, Wen-Bin He, Rubem Mondaini, Xi-Wen Guan, and Hai-Qing Lin. Scaling of energy and power in a large quantum battery-charger model. *Phys. Rev. Res.*, 4:043150, Nov 2022. doi:10.1103/PhysRevResearch.4.043150. URL <https://link.aps.org/doi/10.1103/PhysRevResearch.4.043150>.
- ⁵⁷ Yan Hong, Xianfei Qi, Ting Gao, and Fengli Yan. Detection of multipartite entanglement via quantum fisher information. *Europhysics Letters*, 134(6):60006, sep 2021. doi:10.1209/0295-5075/134/60006. URL <https://dx.doi.org/10.1209/0295-5075/134/60006>.
- ⁵⁸ Federico Dell’Anna, Sunny Pradhan, Cristian Degli Esposti Boschi, and Elisa Ercolessi. Quantum fisher information and multipartite entanglement in spin-1 chains. *Phys. Rev. B*, 108:144414, Oct 2023. doi:10.1103/PhysRevB.108.144414. URL <https://link.aps.org/doi/10.1103/PhysRevB.108.144414>.
- ⁵⁹ George Mathew, Saulo L. L. Silva, Anil Jain, Arya Mohan, D. T. Adroja, V. G. Sakai, C. V. Tomy, Alok Banerjee, Rajendar Goreti, Aswathi V. N., Ranjit Singh, and D. Jaiswal-Nagar. Experimental realization of multipartite entanglement via quantum fisher informa-

- tion in a uniform antiferromagnetic quantum spin chain. *Phys. Rev. Res.*, 2:043329, Dec 2020. doi:10.1103/PhysRevResearch.2.043329. URL <https://link.aps.org/doi/10.1103/PhysRevResearch.2.043329>.
- ⁶⁰ Yuguo Su, Zhijie Sun, Yiyang Yan, Hengyan Wang, Junyan Luo, Tiantian Ying, Hongbin Liang, and Yi-Xiao Huang. Dynamical multipartite entanglement in a generalized tavis-cummings model with xy spin interaction. *Phys. Rev. A*, 111:052415, May 2025. doi:10.1103/PhysRevA.111.052415. URL <https://link.aps.org/doi/10.1103/PhysRevA.111.052415>.
- ⁶¹ Philipp Hyllus, Wiesław Laskowski, Roland Krischek, Christian Schwemmer, Witlef Wieczorek, Harald Weinfurter, Luca Pezzé, and Augusto Smerzi. Fisher information and multiparticle entanglement. *Phys. Rev. A*, 85:022321, Feb 2012. doi:10.1103/PhysRevA.85.022321. URL <https://link.aps.org/doi/10.1103/PhysRevA.85.022321>.
- ⁶² Géza Tóth. Multipartite entanglement and high-precision metrology. *Phys. Rev. A*, 85:022322, Feb 2012. doi:10.1103/PhysRevA.85.022322. URL <https://link.aps.org/doi/10.1103/PhysRevA.85.022322>.